Direct Synthesis of Well-Ordered and Unusually Reactive FeSBA-15 Mesoporous Molecular Sieves

A. Vinu,*,† Dhanshri P. Sawant,§ K. Ariga,‡ K. Z. Hossain,‡ S. B. Halligudi,§ M. Hartmann,# and M. Nomura||

International Center for Young Scientists, National Institute for Materials Science, 1-1, Namiki, Tsukuba, Ibaraki 305-0044, Japan, Inorganic Chemistry & Catalysis Division, National Chemical Laboratory, Pune 411 008, India, Advanced Materials Laboratory, National Institute for Materials Science, 1-1, Namiki, Tsukuba, Ibaraki 305-0044, Japan, Department of Chemistry, University of Kaiserslautern, Kaiserslautern 67663, Germany, and Photon Factory, High Energy Accelerator Research Organization, Tsukuba, Japan

Received April 26, 2005. Revised Manuscript Received June 1, 2005

Large-pore hexagonal SBA-15 molecular sieves partially substituted with iron(III) have been synthesized for the first time in highly acidic media. The degree of iron(III) incorporation into SBA-15 can easily be controlled by a simple adjustment of the molar ratio of water and hydrochloric acid. All the materials have been characterized by XRD, N_2 adsorption, UV−Vis DRS, ESR, and XANES spectroscopy. The characterization of the FeSBA-15 materials by UV−Vis DRS, ESR, and XANES spectroscopies suggests that the iron atoms are highly dispersed and mostly occupy isolated tetrahedral sites. XANES studies revealed that the proportion of tetrahedrally coordinated Fe atoms decreases with decreasing n_{Si}/n_{Fe} ratios. Benzylation of benzene (or substituted benzenes) using benzyl chloride as the alkylating agent over FeSBA-15 with different n_{Si}/n_{Fe} ratios was investigated as was the same reaction using AlSBA-15 as catalyst. The influence of parameters such as reaction temperature, reactant feed ratio, and the presence of electron-donating substituents on the activity and selectivity of AlSBA-15 was studied. Under optimized reaction conditions, the FeSBA-15 catalyst showed a superior catalytic performance in the benzylation of benzene and other aromatics using benzyl chloride, with a clean conversion of benzyl chloride to the monoalkylated product (100% selectivity) with a very high rate constant when compared to other mesoporous materials such as AlSBA-15 and FeHMS. Interestingly, use of FeSBA-15(21) resulted in quantitative conversion of benzyl chloride with a high rate constant of 2420.5×10^{-4} min^{-1} under the optimized reaction conditions.

Introduction

Highly ordered large-pore mesoporous silica SBA-15, which has considerably thicker pore walls than MCM-41, was recently synthesized in highly acidic media using an amphiphilic triblock copolymer as the structure-directing agent.[1] The incorporation of trivalent atoms (Al, Fe, or Ga) into the walls of the zeolite lattice or mesoporous silica creates Brønsted acid sites and allows preparation of materials of various acidity which possess different catalytic and adsorptive properties.[2−10] Among these, iron(III)-substituted MCM-41 has received much attention because of its redox properties and unusual activity in alkylation[2] and oxidation reactions.[4,9−11] Although the MCM-41 materials show interesting catalytic properties, they have very low mechanical and hydrothermal stabilities because of their thinner pore walls. SBA-15 contains thicker pore walls and has better hydrothermal stability than MCM-41.[1] However, incorporation of metal ions into the framework of SBA-15 is very difficult because of the strongly acidic synthesis conditions.[12] Several studies have dealt with incorporation of metal ions into SBA-15 using solely postsynthetic grafting methods.[12] During preparation of the materials by these methods metal oxides are often formed in the channels and this may reduce the specific surface area, pore volume, and pore diameter or have a negative effect on the catalysis.[13] Very recently, Vinu et al. reported the direct incorporation of large quantites of

* To whom correspondence should be addressed. Phone: +81-29-851-3354 (ext. 8679). Fax: +81-29-860-4706. E-mail: vinu.ajayan@nims.go.jp.
† International Center for Young Scientists, National Institute for Materials Science.
§ National Chemical Laboratory.
‡ Advanced Materials Laboratory, National Institute for Materials Science.
|| High Energy Accelerator Research Organization.
University of Kaiserslautern.

(1) Zhao, D.; Huo, Q.; Feng, J.; Chmelka, B. F.; Stucky, G. D. *J. Am. Chem. Soc.* **1998**, *120*, 6024.
(2) He, N.; Bao, S.; Xu, Q. *Appl. Catal., A* **1998**, *169*, 29.
(3) Tuel, A.; Acron, I.; Millet, J. M. M. *J. Chem. Soc., Faraday Trans. B* **1998**, *94*, 3501. Tuel, A.; Gontier, S. *Chem. Mater.* **1996**, *8*, 114.
(4) Corma, A.; Fornés, V.; Navarro, M. T.; Pérez-Pariente, J. *J. Catal.* **1994**, *148*, 569.
(5) Vinu, A.; Murugesan, V.; Böhlmann, W.; Hartmann, M. *J. Phys. Chem. B* **2004**, *108*, 11496.
(6) Vinu, A.; Murugesan, V.; Hartmann, M. *J. Phys. Chem. B* **2004**, *108*, 7323.
(7) Vinu, A.; Murugesan, V.; Tangermann, O.; Hartmann, M. *Chem. Mater.* **2004**, *16*, 3056.
(8) Vinu, A.; Hartmann, M. *Chem. Lett.* **2004**, *33*, 588.
(9) Vinu, A.; Usha Nandhini, K.; Murugesan, V.; Böhlmann, W.; Umamaheswari, V.; Pöppl, A.; Hartmann, M. *Appl. Catal., A* **2004**, *265*, 1.
(10) Vinu, A.; Krithiga, T.; Murugesan, V.; Hartmann, M. *Adv. Mater.* **2004**, *16*, 1817.
(11) Parvulescu, V.; Su, B.-L. *Catal. Today* **2001**, *69*, 315.
(12) Vinu, A.; Murugesan, V.; Hartmann, M. *Chem. Mater.* **2003**, *15*, 1385. Luan, Z.; Hartmann, M.; Zhao, D.; Zhou, W.; Kevan, L. *Chem. Mater.* **1999**, *11*, 1621.
(13) Murugavel, R.; Roesky, H. W. *Angew. Chem., Int. Ed.* **1997**, *109*, 44491.

10.1021/cm050883z CCC: $30.25
Published on Web 09/17/2005

Al(III) into the SBA-15 framework by a simple adjustment of the molar ratio of water and hydrochloric acid of the synthesis medium.[5] They also found that the pore diameter of the AlSBA-15 materials can be easily controlled by variation of the synthesis temperature. Here, we extend that synthetic methodology by the preparation of mesoporous ferrisilicate materials (FeSBA-15).

The liquid-phase benzylation of benzene and other aromatic compounds using benzyl chloride (hereafter referred to as BC) or benzyl alcohol is important for the production of diphenylmethane (DPM) and substituted diphenylmethanes, which are important industrially as intermediates for pharmaceuticals and other fine chemicals.[14−17] Industrial syntheses of DPMs are carried out using conventional strong acid catalysts, such as $AlCl_3$, $FeCl_3$, BF_3, $ZnCl_2$, and H_2SO_4 under homogeneous conditions.[14−18] However, those catalysts pose problems of toxicity, handling hazards, difficulty in separation and recovery of the catalyst, and product isolation. Other issues include difficulties in disposal of large amounts of acidic effluents, corrosion, and their requirement in stoichiometric amounts. Thus, there has been much interest in replacing these homogeneous catalysts with heterogeneous solid acid catalysts possessing high activity for Friedel−Crafts type reactions, and which can be separated easily from the reaction mixture and reused. Earlier studies indicated that strongly acidic zeolite catalysts, such as HY and H−ZSM-5, show poor activity in the benzylation reaction because of diffusion limitations inflicted by their microporous network.[19,20] However, partial substitution of Al(III) by Fe(III) or Ga(III) in H−ZSM-5 greatly improved the catalyst performance in the benzylation process.[20,21] Choudhary et al. have reported that iron-pillared clays were the most efficient catalysts, giving quantitative conversions using greatly reduced amounts of catalysts and in shorter reaction times.[22] Solid superacids based on sulfated zirconia also show poor activity in the benzylation of benzene and other aromatic compounds.[23] Choudhary et al. have also reported that $AlCl_3$ supported on Si−MCM-41 showed poor catalytic activity for the benzylation of benzene, whereas supported $FeCl_3$, $GaCl_3$, and $InCl_3$ were highly active.[24−26] Conversely, Hu et al. found that $AlCl_3$/MCM-41 showed higher activity compared to other metal chloride supported mesoporous catalysts, such as $ZnCl_2$/MCM-41, $FeCl_3$/MCM-41, $CuCl_2$/MCM-41, and $NiCl_2$/MCM-41.[27] However, the immobilized metal chloride blocks the pores, either partially or fully, thereby reducing the specific surface area, pore volume, and pore diameter, and can also play a negative role in the catalysis by leaching, catalyst poisoning, or obstruction of the active sites.

In this paper, we report the direct synthesis and characterization of iron-substituted SBA-15 materials with various $n_{Si/Fe}$ ratios and their catalytic performance in the benzylation of benzene and substituted benzenes. Our main approach has been to incorporate iron atoms into SBA-15 materials by a simple adjustment of the pH of gel mixtures above the isoelectric point of silica (pH ∼2) so that negatively charged silica species can easily interact with the positively charged iron hydroxo complexes $[Fe(OH)_2^+]$, resulting in incorporation of larger quantities of Fe into the SBA-15 mesoporous silica matrix. It was also found that this catalyst registered a quantitative conversion and a very high selectivity with small amounts of catalyst and relatively short reaction times.

Experimental Section

Materials. Ferric nitrate nonahydrate and tetraethyl orthosilicate (Merck) were used as the source for iron(III) and silicate, respectively. Triblock copolymer poly(ethylene glycol)-*block*-poly(propylene glycol)-*block*-poly(ethylene glycol) (**P**luronic **P**123, molecular weight = 5800, $EO_{20}PO_{70}EO_{20}$) (Aldrich) was used as the structure-directing template. Benzene (*caution: poisonous and carcinogenic*), benzyl chloride, and diphenylmethane were purchased from Aldrich.

Preparation of the Catalysts. FeSBA-15 materials with various $n_{Si/Fe}$ ratios were prepared using the following procedure: amphiphilic triblock copolymer Pluronic P123 (4 g) was dispersed in 30 g of water and stirred for 4 h; 70 mL of 0.29 M HCl was added and the mixture stirred for 2 h (pH = ca. 2.2). Then 9.0 g of tetraethyl orthosilicate (TEOS) and the appropriate amount of ferric nitrate were added directly to the homogeneous solution with stirring. The resulting gel was aged at 40 °C for 24 h and finally warmed at 100 °C for 48 h. The molar composition of the gel synthesis mixture was 1:0.026−0.1:0.016:0.46:127 TEOS:Fe_2O_3:P123:HCl:H_2O. The samples were labeled FeSBA-15(*x*) where *x* denotes the n_{Si}/n_{Fe} molar ratio. Pure siliceous SBA-15 was synthesized using the same procedure (1:0.016:5.54:190 TEOS:P123:HCl:H_2O) in the absence of iron. After synthesis, the solids obtained were calcined in flowing air at 540 °C to decompose the triblock copolymer. Preparation of FeSBA-15 was also attempted using the same molar composition of the gel as that used for preparation of pure siliceous SBA-15. It is important to note that FeSBA-15 prepared by the latter method contains no Fe atoms in the final product as indicated by AAS measurements because of the strong repulsive interaction between positively charged silica and iron hydroxo complexes and the high solubility of the iron source in a highly acidic medium (pH below 2).

Characterization. The powder X-ray diffraction patterns of FeSBA-15 samples were collected using a Rigaku diffractometer with Cu Kα (λ = 0.154 nm) radiation. The diffractograms were recorded in the 2θ range of 0.8−10° with a 2θ step size of 0.01° and a step time of 10 s. Nitrogen adsorption and desorption isotherms were measured at 77 K on a Quantachrome Autosorb 1 sorption analyzer. The samples were outgassed for 3 h at 250 °C under vacuum in the degas port of the adsorption analyzer. Specific

(14) Olah, G. A. *Friedel−Crafts Chemistry*, Wiley: New York, 1973.
(15) Commandeur, R.; Berger, N.; Jay, P.; Kervennal, J. EP 0442986, 1991.
(16) Bastock, T. W.; Clark, J. H. *Speciality Chemicals*, Elsevier: London, 1991.
(17) Khadilkar, B. M.; Borkar, S. D. *Chem. Technol. Biotechnol.* **1998**, *71*, 209.
(18) Olah, G. A.; Prakash, G. K. S.; Sommer, J. *Superacids*; Wiley-Interscience: New York, 1985.
(19) Coq, B.; Gourves, V.; Figueras, F. *Appl. Catal. A* **1993**, *100*, 69.
(20) Choudhary, V. R.; Jana, S. K.; Kiran, B. P. *Catal. Lett.* **1999**, *59*, 217.
(21) Choudhary, V. R.; Jana, S. K. *Appl. Catal., A* **2002**, *224*, 51.
(22) Choudary, B. M.; Kantam, M. L.; Sateesh, M.; Rao, K. K.; Shanthi, P. L. *Appl. Catal., A* **1997**, *149*, 257.
(23) Koyande, S. N.; Jaiswal, R. G.; Jayaram, R. V. *Ind. Eng. Chem. Res.* **1998**, *37*, 908.
(24) Choudhary, V. R.; Jana, S. K.; Kiran, B. P. *Catal. Lett.* **2000**, *64*, 223.
(25) Choudhary, V. R.; Jana, S. K. *J. Mol. Catal. A: Chem.* **2002**, *180*, 267.
(26) Choudhary, V. R.; Jana, S. K.; Mamman, A. S. *Microporous Mesoporous Mater.* **2002**, *56*, 65.
(27) Hu, X.; Chuah, G. K.; Jaenicke, S. *Appl. Catal., A* **2001**, *217*, 1.

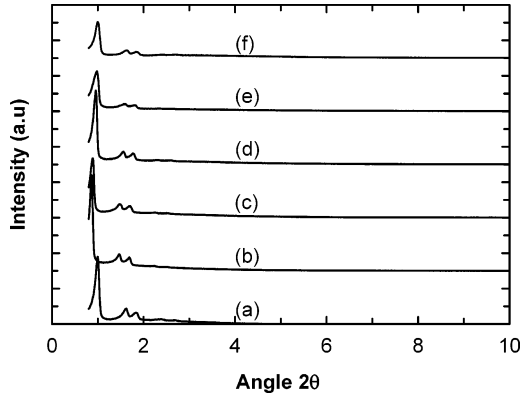

Figure 1. XRD powder patterns of calcined FeSBA-15 with differing n_{Si}/n_{Fe} ratios: (a) SBA-15, (b) FeSBA-15(21), (c) FeSBA-15(55), (d) FeSBA-15(96), (e) FeSBA-15(152), and (f) FeSBA-15(∞).

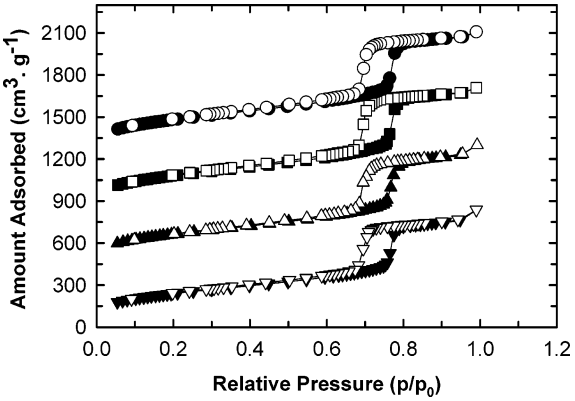

Figure 2. Nitrogen adsorption isotherm (adsorption: closed symbols; desorption: open symbols) of FeSBA-15 materials with different n_{Si}/n_{Fe} ratios: (●) FeSBA-15(21), (■) FeSBA-15(55), (▲) FeSBA-15(96), and (▼) FeSBA-15(152). The isotherms have been offset (in 400 unit steps) for clarity.

surface area was calculated using the BET model. UV−Vis diffuse reflectance spectra were measured with a Perkin-Elmer Lambda 18 spectrometer equipped with a Praying-Mantis diffuse reflectance attachment using $BaSO_4$ as reference. Elemental analysis was performed using an Analyst AA 300 spectrometer. X-band ESR (9.7 GHz) spectra were recorded at 77 K using a BRUKER ESP 300E spectrometer. The static Fe K-edge XANES measurements were carried out at BL-9A (Photon Factory, High Energy Accelerator Research Organization, Tsukuba, Japan) using a Si(111) double-crystal monochromator and ionization chambers. The double-crystal monochromator of Bl-09A was further detuned to 60% of the maximum intensity at the absorption edge. The angle of the monochromator was calibrated using iron foil.

Catalytic Studies. Anhydrous A.R. grade chemicals were used without further purification. The liquid-phase benzylation of benzene with benzyl chloride (BC) was carried out in a 50 mL two-necked flask equipped with a condenser and a septum. The temperature of the reaction vessel was maintained using an oil bath. In a typical run, benzene and BC were added in the required molar ratio to the activated catalyst. The catalysts were activated at 773 K in air for 4 h with a flow rate of 50 mL/min and cooled to room temperature prior to their use in the reaction. The reaction mixture was magnetically stirred and heated to the required temperature under atmospheric pressure. Samples were withdrawn at regular intervals and analyzed using a gas chromatograph (HP-6890) equipped with a FID detector and a capillary column. The products were also identified by GC-MS (HP-5973) analysis. Since benzene was used in excess, conversion was calculated based on the benzylating reagent, i.e., BC.

Results and Discussion

Characterization of FeSBA-15. Figure 1 shows the powder XRD patterns of pure siliceous SBA-15 and FeSBA-15 samples after calcination. The relatively well-defined patterns are similar to SBA-15 materials as described by Zhao et al.[1] All four reflections (100), (110), (200), and (210) are resolved and can be indexed in the hexagonal space group *p*6*mm*. The existence of (200) and (210) peaks indicates an excellent textural uniformity of the material. The length of the hexagonal unit cell a_0 is calculated using the formula $a_0 = 2d_{100}/\sqrt{3}$. The unit cell parameter of the materials increases with increasing Fe content, suggesting the presence of Fe atoms in the framework. A similar result has also been reported in the metal-substituted mesoporous materials.[28] Additionally, it should be noted that the wall thickness ($W = a_o - d_p$) of the FeSBA-15 materials increases with increasing Fe content. Moreover, the intensities of the XRD peaks of FeSBA-15 materials are greater than that of the pure silica SBA-15 sample. This can be attributed to the presence of nitrate ions (from the Fe source, ferric nitrate) in the gel synthesis mixture, which should catalyze the condensation of silica species and assist the formation of thicker pore walls and a well-ordered structure.[29,30]

The incorporation of Fe into the walls of SBA-15 has a significant effect on the specific surface area and pore volume of the materials (Figure 2). All isotherms are of type IV, according to the IUPAC classification, and exhibit an H1 type broad hysteresis loop, which is typical of large-pore mesoporous solids. As the relative pressure increases ($p/p_0 > 0.6$), all isotherms exhibit a sharp step characteristic of capillary condensation of nitrogen within uniform mesopores, where the p/p_0 position of the inflection point correlates with the diameter of the mesopore. Since SBA-15 has a hexagonal arrangement of mesopores connected by smaller micropores, it is clear that the broad hysteresis loop in the isotherms of FeSBA-15 reflects the long mesopores, which limit the emptying and filling of the accessible volume. The amount of nitrogen adsorbed decreases with increasing Fe content in FeSBA-15. With increasing metal content, the pore volume decreases from 1.35 to 1.18 cm^3/g and the specific surface area declines from 1024 to 880 $m^2/$ g (Table 1). This is attributed to a slight reduction of the sample quality with increasing metal content. A similar behavior has also been observed in metal-substituted MCM-41 materials.[31] However, the reduction in the pore volume with increase of Fe content might be due to the blocking of some of the micropores of FeSBA-15 and/or the mesoporous channels with iron oxide species during calcination.

UV−Vis spectroscopy has been used extensively to characterize the nature and coordination of Fe^{3+} ions in Fe-substituted molecular sieves.[32,33] Figure 3 shows UV−Vis DRS spectra of calcined FeSBA-15 samples with different

(28) Cheng, C.-F.; Klinowski, J. *J. Chem. Soc., Faraday Trans. B* **1996**, *92*, 289.
(29) Lin, H.-P.; Mou, C.-P.; Liu, S.-B. *J. Phys. Chem B* **2000**, *104*, 7885;
(30) Israelachvili, J. N.; Mitchell, D. J.; Ninham, B. W. *J. Chem. Soc., Faraday Trans. B* **1976**, *72*, 1525.
(31) Kruk, M.; Jaroniec, M.; Sayari, A. *Langmuir* **1999**, *15*, 5683.

Table 1. Textural Properties of SBA-15 and FeSBA-15 Samples

catalyst	n_{Si}/n_{Fe} gel	n_{Si}/n_{Fe} AAS	a_o/nm	$A_{BET}/\pm 5$ m^2/g	d_p/nm	V_p/cm^3 g^{-1}	$W = a_0 - d_p$
SBA-15			10.1	910	9.2	1.25	0.9
FeSBA-15(21)	5	21	11.9	880	9.3	1.18	2.6
FeSBA-15(55)	7	55	11.5	960	9.3	1.29	2.2
FeSBA-15(96)	9	96	10.6	1024	9.3	1.35	1.3
FeSBA-15(152)	19	152	10.5	1024	9.3	1.35	1.2
FeSBA-15()	0	0	10.32	920	9.2	1.20	1.1

n_{Si}/n_{Fe} ratios. A broad band between 43000 and 28000 cm^{-1} centered at 37735 cm^{-1} is observed in all samples. The intensity of this band increases monotonically with increasing Fe content. This band has been assigned to a low-energy charge transfer between the oxygen ligands and the central Fe^{3+} ion in tetrahedral symmetry. A similar band was also reported in ferrisilicate materials containing tetrahedrally coordinated iron species.[33] This indicates that iron still exists in the tetrahedral coordination environment even after calcination. However, for the sample Fe−SBA-15(21) a change in color from white to pale orange was observed and a broad absorption band in the visible region was detected probably due to the presence of Fe(II) or Fe_2O_3 species[34] while the formation of Fe_2O_3 was not observed for samples with lower Fe content.

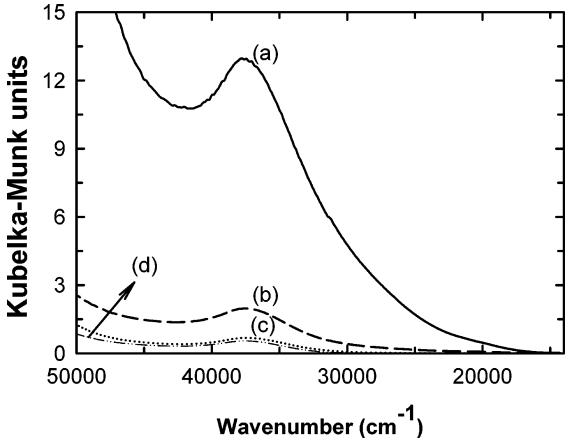

Figure 3. UV−Vis DRS spectra of calcined FeSBA-15 samples: (a) FeSBA-15(21), (b) FeSBA-15(55), (c) FeSBA-15(96), and (d) FeSBA-15-(152).

X-band ESR spectra of the calcined FeSBA-15(55) and FeSBA-15(96) samples show two peaks which are centered at $g = 2.0$ and 4.3 (Figure 4). Similar spectra were previously reported by Bordiga et al. and Goldfarb et al. for iron-substituted mesoporous and microporous silicates.[33,34] Both groups proposed different interpretations for their ESR results. Bordiga et al. suggested that the ESR signal at $g = 4.3$ originating from the middle Kramers doublet could be assigned to tetrahedrally coordinated iron species (Fe^{3+}) in the framework while the signal at $g = 2.0$ is assigned to small extraframework Fe^{3+} ions.[33] In contrast, Goldfarb et al. assigned the ESR signal at $g = 4.3$ to framework defect sites with terminal oxygen in the zeolitic materials. This was further supported by the disappearance of the signal with increasing iron(III) concentration in the zeolite lattice. They also suggested the absence of the $g = 4.3$ signal in the ESR spectrum does not exclude the possibility of framework subsitution. Further, the same authors reported that the ferrosilicate materials with tetrahedral coordinated Fe^{3+} species, which are proved by the various spectroscoic techniques such as UV−Vis DRS and EXAFS, gave the ESR signal at $g = 2.0$. Park et al. also assigned the $g = 2$ signal of Fe in FAPO-5 to tetrahedral framework Fe^{3+}.[35] Thus, we assumed that the ESR signal at $g = 2.0$ and 4.3 could be assigned to tetrahedral coordinated Fe^{3+} and extraframewrok Fe−O clusters, respectively. However, detailed re-evaluation of the assignment of these ESR signals is necessary and needs further study. It should be noted that FeSBA-15(21) shows a broad ESR signal between $g = 1.9$ and $g = 3.2$. This broad signal could be due to the proximal iron centers in the materials. Thus, it is difficult to assign this signal either to the tetrahedral or octahedral coordination of Fe. Tuel et al. have reported the same type of broad signal in FeHMS materials and suggested that it can be assigned to dispersed iron oxide particles inside the mesoporous channels.[3]

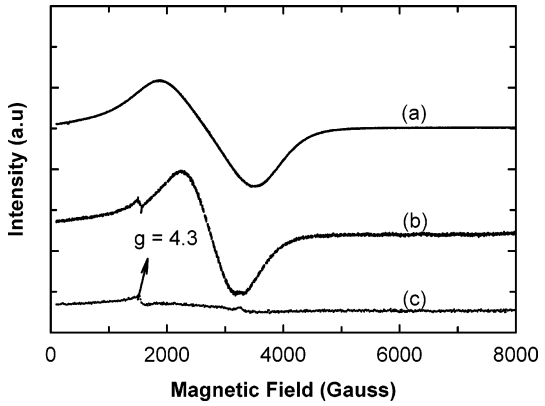

Figure 4. ESR spectra of calcined FeSBA-15 with different n_{Si}/n_{Fe} ratios: (a) FeSBA-15(21), (b) FeSBA-15(55), and (c) FeSBA-15(96).

The oxidation and coordination state of Fe in the FeSBA-15 catalysts were also studied by X-ray absorption spectroscopy. It has been reported that the pre-edge feature of Fe in the X-ray absorption near-edge structure (XANES) is very sensitive to the local coordination status.[34] Also, the local environment of the Fe species and its electronic structure can be easily obtained from the position, intensity, and shape of the pre-edge peaks in the XANES spectrum. Figure 5 shows the near-edge region of the XANES spectra of FeSBA-15 catalysts with different n_{Si}/n_{Fe} ratios. All the

(32) Wang, A.; Zhang, Q.; Shishido, T.; Takehira, K. *J. Catal.* **2002**, *209*, 186.
(33) Bordiga, S.; Buzzoni, R.; Geobalda, F.; Lamberti, C.; Giomello, E.; Zecchina, A.; Leofani, G.; Petrini, G.; Tozzola, G.; Vlaic, G. *J. Catal.* **1996**, *148*, 486.
(34) Goldfarb, D.; Bernardo, M.; Strohmaier, K. G.; Vaughan, D. E. W.; Thomann, H. *J. Am. Chem. Soc*. **1994**, *116*, 6344.
(35) Park, J. W.; Chon, H. *J. Catal.* **1992**, *133*, 159.

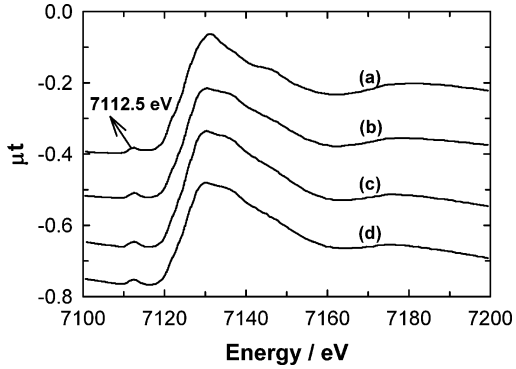

Figure 5. Fe K-edge XANES spectra for FeSBA-15 with different n_{Si}/n_{Fe} ratios: (a) FeSBA-15(21), (b) FeSBA-15(55), (c) FeSBA-15(96), and (d) FeSBA-15(152).

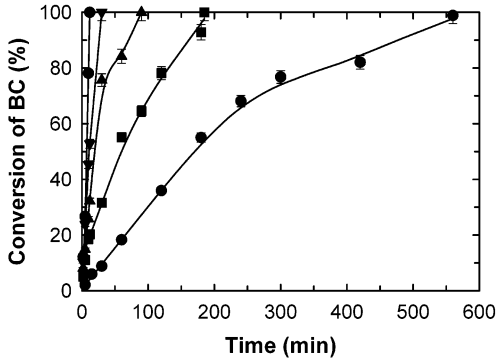

Figure 6. Benzyl chloride conversion in the benzylation of benzene over different catalysts at 343 K as a function of time, benzene-to-benzyl chloride ratio 15, and amount of catalyst 30 mg: (●) FeSBA-15(21), (■) FeSBA-15(55), (▲) FeSBA-15(96), (d) (▼) FeSBA-15(152), and (◆) AlSBA-15-(45).

samples show a single well-defined pre-edge peak which is centered around 7112.5 eV. This pre-edge peak has been assigned to the 1s → 3d transition of the tetrahedrally coordinated Fe^{3+}. This transition is Laporte forbidden for octahedral coordination. However, a pre-edge peak with very low intensity is often observed for samples containing a distorted octahedrally coordinated Fe atom. It has also been reported that the pre-edge peak intensity is directly related to the percentage of Fe^{3+} with tetrahedral coordination. The coordination state of the Fe atom changes as follows as the intensity of the pre-edge peak decreases: tetrahedral → distorted tetrahedral → pyramidal→ distorted octahedral → octahedral.[34] It can be seen from Figure 5 that the intensity of the pre-edge peak decreases with increasing Fe content, indicating that the amount of tetrahedrally coordinated Fe atoms decreases with decreasing n_{Si}/n_{Fe} ratios. The intensity of the pre-edge peak for FeSBA-15(21) is lower than that for other FeSBA-15 samples, indicating that a small amount of octahedrally coordinated Fe species is located inside the channels of FeSBA-15(21). This result supports the conclusion of the UV−vis and ESR analysis of FeSBA-15.

Catalytic Studies. The conversion of benzyl chloride (BC) in the benzylation of benzene over an FeSBA-15 catalyst with different n_{Si}/n_{Fe} ratios or over AlSBA-15 is shown in Figure 6. The products obtained are diphenylmethane (DPM) and the isomers of dibenzylbenzene (DBB), 1,4-DBB, 1,3-DBB, and 1,2-DBB. All catalysts showed 100% conversion and 87−100% selectivity for DPM during reaction times of 12−540 min. For all the catalysts, the BC conversion

Table 2. Properties of the Catalysts in the Benzylation of Benzene Using Benzyl Chloride at 343 K[a]

catalyst	time[c]/min	selectivity/% DPM[d]	selectivity/% others	rate constant $k_a\,10^{-4}/\text{min}^{-1}$
FeSBA-15(152)[b]	185	100		117.5
FeSBA-15(96)[b]	90	100		522.7
FeSBA-15(55)[b]	30	94.5	5.5	677.1
FeSBA-15(21)[b]	12	87.1	12.9	2420.5
FeHMS(50)[f]	245	100	0	40.8
AlSBA-15(45)	540[e]	100	18.8	11.5

[a] Reaction conditions: benzene:benzyl chloride = 15:1 (molar ratio). [b] Amount of catalyst: 30 mg. [c] Time required for complete conversion of benzyl chloride. [d] Diphenylmethane. [e] 39.6% BC conversion. [f] Amount of catalyst: 100 mg.

increased linearly with time up to a conversion of 60−70%. It is interesting to note that FeSBA-15(96) gave 100% conversion of benzyl chloride and 100% selectivity for DPM within 90 min of the reaction time whereas FeSBA-15(21) showed 100% conversion of benzyl chloride and 87.1% selectivity for DPM after 12 min. By contrast, AlSBA-15-(45) registered only 39.6% BC conversion, which is much lower than those obtained with the FeSBA-15 catalysts after 540 min of reaction under the same reaction conditions. The benzylation activity of Fe−HMS(20) catalyst was also compared with those of the FeSBA-15 catalysts. It can be seen from Table 2 that mesoporous Fe−HMS-50[36] (benzene-to-catalyst ratio = 220) showed a similar reactivity to the FeSBA-15 catalysts (benzene-to-catalyst ratio = 90), although a 100% BC conversion and 100% selectivity for DPM at 348 K could be achieved in 245 min. It is also important to note that the amounts of AlSBA-15(45) and Fe−HMS-(50) catalysts used were 3 times greater than the amounts of FeSBA-15 catalysts used in the reaction. Among the catalysts studied, FeSBA-15(96) was found to be a more active and selective catalyst for the conversion of benzyl chloride and formation of DPM. The activity of the catalysts, in terms of conversion of benzyl chloride and reaction time, decreases in the following order: FeSBA-15(21) > FeSBA-15(55) > FeSBA-15(96) > FeSBA-15(152) > AlSBA-15(45).

The rate data for the benzylation of benzene reaction in excess benzene over FeSBA-15 and AlSBA-15 catalysts can be fitted well to a pseudo-first-order rate law:

$$\log[1/(1-x)] = (k_a/2.303)\,(t - t_0)$$

where k_a is the apparent rate constant, x the fractional conversion of benzyl chloride, t the reaction time, and t_0 the induction period corresponding to the time required for reaching the equilibrium temperature. A plot of $\log[1/1 - x]$ versus $(t - t_0)$ gives a linear plot over a range from 10 to 90%. The apparent rate constants for the different catalysts declines in the following order: FeSBA-15(21) > FeSBA-15(55) > FeSBA-15(92) > FeSBA-15(152) > FeHMS(50)[36] > AlSBA-15(45). The apparent rate constant for the benzylation reaction over FeSBA-15(21) is $2420.5 \times 10^{-4}\ \text{min}^{-1}$ and that of FeHMS(50) is $40.8 \times 10^{-4}\ \text{min}^{-1}$ while AlSBA-15(45) registers an apparent rate constant of only $11.5 \times 10^{-4}\ \text{min}^{-1}$.

(36) Bachari, K.; Millet, J. M. M.; Benaichouba, B.; Cherifi, O.; Figueras, F. *J. Catal.* **2004**, *221*, 55.

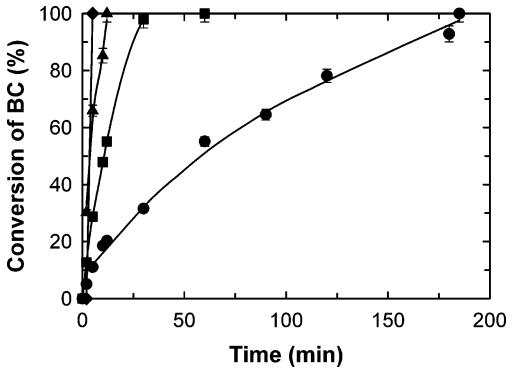

Figure 7. Effect of reaction temperature on the conversion of benzyl chloride in the benzylation of benzene reaction over FeSBA-15(152) at (●) 343, (■) 353, (▲) 358, and (◆) 363 K.

Table 3. Influence of Reaction Temperature on the Catalytic Activity of the Benzene Benzylation Reaction over FeSBA-15(152) Catalyst[a]

		selectivity/%		
temperature/K	time[b]/min	diphenylmethane	1,4-DBB	rate constant k_a 10^{-4}/ min^{-1}
343	185	100		117.5
353	30	98.60	1.40	829.1
358	12	98.50	1.40	1911.5
363	2	98.40	1.6	

[a] Reaction conditions: benzene:BC = 15:1 (molar ratio). Amount of catalyst = 30 mg (1 wt % of total reaction mixture). [b] Time required for the complete conversion of benzyl chloride.

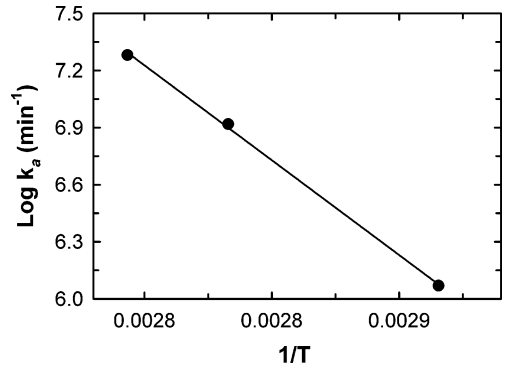

Figure 8. Arrhenius plot of log k_a as a function of ($1/T$) for the benzylation benzene reaction over FeSBA-15(152) catalyst.

The effect of reaction temperature on the benzylation of benzene over FeSBA-15(152) in the range 343−363 K was also studied. The benzyl chloride conversion as a function of reaction time and at various reaction temperatures is presented in Figure 7. The product selectivities are given in Table 3. The results show that the performance of the catalyst increases substantially with increasing reaction temperature. Table 3 and Figure 7 illustrate that the time for 100% benzyl chloride conversion decreased from 185 min at 343 K to 2 min at 363 K, while the apparent rate constant k_a increased from 117.5×10^{-4} min^{-1} at 343 K to 1911.5×10^{-4} min^{-1} at 358 K. It is also significant to note that there was only a slight change in the selectivity for DPM and at least a 98.4 to 100% selectivity for DPM was achieved at all the reaction temperatures used in this study. The first-order rate constants calculated from these curves give an Arrhenius plot (Figure 8) and indicate a value of the activation energy for the FeSBA-15(152) catalyst of 190.94 kJ/mol. The effect of catalyst loading on conversion and selectivity was also studied between 0.05 and 3 wt % of the total reaction mixture over FeSBA-15(152) at a reaction temperature of 343 K and with a benzene-to-BC feed ratio of 15. An increase in catalyst loading from 0.5 to 3 wt % is associated with a decrease in reaction time from 320 to 20 min for 100% benzyl chloride conversion and a decreased selectivity for DPM from 100 to 98.2%, respectively (Table 1S, see Supporting Information).

Table 4. Influence of Stoichiometric Ratio of Benzene to Benzyl Chloride on the Benzene Benzylation Reaction over FeSBA-15(152) at a Reaction Temperature of 343 K[a]

		selectivity/%			
			isomers of DBB		
benzene-to-BC molar ratio	time[b]/min	DPM	1,2-DBB	1,3-DBB	1,4-DBB
5	300	70.8	5.2	2.9	21.1
7.5	245	82.7	3.6	1.5	12.2
10	210	92.3	1.5	0.9	5.3
15	185	100	-	-	-

[a] Amount of catalyst = 30 mg (1 wt % of total reaction mixture) [b] Time required for the complete conversion of benzyl chloride.

Table 5. Effect of the Presence of Electron-Donating Substituents on Benzene in the Benzylation Reaction over FeSBA-15(152) at a Reaction Temperature of 343 K[a]

aromatic compound	time[b]/min	major product selectivity/%
benzene	185	100[c]
toluene	210	89.80[d]
p-xylene	300	100[e]
mesitylene	345	100[f]
anisole	360	100[g]

[a] Substituted benzene-to-BC ratio = 15. Amount of catalyst = 30 mg (1 wt % of total reaction mixture) [b] Time required for the complete conversion of benzyl chloride. [c] Diphenylmethane. [d] 4-Methyl diphenylmethane. [e] 2,5-Dimethyl diphenylmethane. [f] 2,4,6-Trimethyl diphenylmethane. [g] 4-Methoxy diphenylmethane.

The effect of the stoichiometric ratios of benzene to BC in the benzene benzylation reaction was also studied over the FeSBA-15(152) catalyst at a reaction temperature of 343 K. The molar ratio of benzene to BC was varied from 5 to 15 and the product distribution at various benzene-to-BC ratios is shown in Table 4. It was found that both activity and selectivity are influenced drastically by the change of reactant molar ratio. The results show that the time for 100% benzyl chloride conversion decreased from 300 to 185 min when the benzene-to-BC ratio increased from 5 to 15. It can also be seen from Table 4 that the selectivity for DPM increases with increasing benzene content. At a benzene: BC ratio of 15, a selectivity of 100% can be achieved. The increase in BC conversion and DPM selectivity with increasing benzene-to-BC ratio can be attributed to the increased adsorption of benzene over the catalyst surface and higher dilution of BC. It is also interesting to note that the selectivity for DBB decreases with increase of the benzene-to-BC feed molar ratio.

The conversion and product distributions for the benzylation of different aromatic compounds are given in Table 5. The BC conversion decreases in the following order: benzene > toluene > *p*-xylene > mesitylene > anisole. The results indicate that the benzylation activity of the FeSBA-15(45) catalyst is decreased by the presence of electron-donating groups such as methyl or methoxy in the aromatic substrate. This result is opposite to that expected according

to the classical mechanism of the Friedel−Crafts acid-catalyzed benzylation reaction where the benzylation of an aromatic compound is facilitated if one or more electron-donating groups are present in the aromatic ring.[14,37] In this study, the FeSBA-15 catalyst shows a possible poisoning caused by the strong adsorption of the aromatic substrate, and this effect increases when the electron density of the aromatic substrate is increased, resulting in a low activity. A similar effect has also been reported on the acetylation of 2-methoxynaphthalene with acetic anhydride over dealuminated HY zeolites.[38]

To study its heterogeneous nature, a test reaction using the FeSBA-15 catalyst was carried out under the optimized reaction conditions. The reaction was stopped when the conversion reached 64.5% and the catalyst was then removed by filtration. The filtrate was immediately reused in the benzylation of benzene reaction and it was found that there was no increase in substrate conversion. The filtered catalyst was also reused with fresh reagents and no loss in its catalytic activity was found. When the reaction was carried out with pure siliceous SBA-15 catalyst, FeSBA-15(∞), or without catalyst, no benzyl chloride conversion was found. These data are in agreement with an absence of catalyst leaching and a purely heterogeneous catalysis. The activity of a regenerated catalyst was tested by filtration of the catalyst from an optimized reaction and then washing three times with A.R. grade acetone followed by drying overnight in an oven at 373 K. The catalyst was subsequently activated at 773 K for 4 h under an air flow and used for the above reaction. The same procedure was repeated two or three times and results of the reaction are given in Table 2S (see Supporting Information). The conversion of BC and the selectivity for DPM did not change even after two or three reaction cycles. Thus, we conclude that the catalytic activity of FeSBA-15 can be maintained even after two or three cycles.

(37) Choudhary, V. R.; Jana, S. K.; Kiran, B. P. *J. Catal.* **2000**, *192*, 257.
(38) Meric, P.; Finiels, A.; Moreau, P. *J. Mol. Catal. A: Chem.* **2002**, *189*, 251.

Conclusions

In conclusion, we have developed a method for the direct synthesis of iron-containing large-pore hexagonal SBA-15 materials where iron ions are mostly tetrahedrally coordinated. The amount of Fe incorporated into SBA-15 can be easily controlled by a simple adjustment of the molar ratio of water to hydrochloric acid. UV−Vis DRS, ESR, and EXAFS studies confirm that the majority of the Fe atoms in FeSBA-15 are in tetrahedral coordination and most probably occupy framework positions. The catalytic activity of this novel catalyst was investigated in the liquid-phase benzylation of benzene reaction. Under the optimized conditions for this reaction, the above catalysts showed superior catalytic performance and recyclability when compared to the AlSBA-15 catalysts.

Acknowledgment. A. Vinu is grateful to the Special Coordination Funds for Promoting Science and Technology from the Ministry of Education, Culture, Sports, Science and Technology of the Japanese Government for the award of a ICYS Research Fellowship. A. V. also thanks Dr. Jonathan P. Hill and Mr. T. Sasaki for the useful discussion.

Supporting Information Available: Acidity measurements and recycling studies of FeSBA-15 catalyst. This material is available free of charge via the Internet at http://pubs.acs.org.

CM050883Z